



IMPLEMENTING MULTI-SCALE AGRICULTURAL INDICATORS EXPLOITING SENTINELS

**VEGETATION FIELD DATA AND PRODUCTION OF
GROUND-BASED MAPS:**

**MERGUELLIL SITE, TUNISIA
8th MARCH AND 3rd MAY 2013**

ISSUE I1.00

EC Proposal Reference N° FP7-311766

Actual submission date : January 2014

Start date of project: 01.11.2012

Duration : 40 months

Name of lead partner for this deliverable: EOLAB



Book Captain: Consuelo Latorre (EOLAB)

Contributing Authors: Jorge Sánchez, Fernando Camacho (EOLAB)

Mehrez Zribi, Hassan Ayari, Bernard Mougnot (CESBIO)
Aicha Chahbi (CESBIO-INAT)

Project co-funded by the European Commission within the Seventh Framework Program (2007-2013)		
Dissemination Level		
PU	Public	X
PP	Restricted to other programme participants (including the Commission Services)	
RE	Restricted to a group specified by the consortium (including the Commission Services)	
CO	Confidential, only for members of the consortium (including the Commission Services)	

DOCUMENT RELEASE SHEET

Book Captain:	C. Latorre	Date: 20.01.2014	Sign. 
Approval:	R. Lacaze	Date: 03.04.2014	Sign. 
Endorsement:	V. Puzzolo	Date:	Sign.
Distribution:			

CHANGE RECORD

Issue/Revision	Date	Page(s)	Description of Change	Release
	20.01.2014	All	First Issue	I1.00

TABLE OF CONTENTS

1.	<i>Background of the Document</i>	8
1.1.	Executive Summary	8
1.2.	Portfolio	8
1.3.	Scope and Objectives.....	9
1.4.	Content of the Document	9
2.	<i>Introduction</i>	10
3.	<i>Study area</i>	11
3.1.	Location	11
3.2.	Description of The Test Site.	12
4.	<i>Ground measurements</i>	13
4.1.	Material and Methods	13
4.2.	Spatial Sampling Scheme	13
4.3.	Content of the Ground Dataset.....	14
5.	<i>Evaluation of the sampling</i>	17
5.1.	Principles.....	17
5.2.	Evaluation Based On NDVI Values.....	17
5.3.	Evaluation Based On Convex Hull: Product Quality Flag.	19
6.	<i>Estimation of the High Resolution Maps</i>	21
6.1.	Imagery	21
6.2.	The Transfer Function	21
6.2.1.	The regression method.....	21
6.2.2.	Band combination	22
6.2.3.	The selected Transfer Function	22
6.3.	The High Resolution Ground Based Maps	24
7.	<i>Conclusions</i>	26
8.	<i>Acknowledgements</i>	27
9.	<i>References</i>	28

LIST OF FIGURES

<i>Figure 1: Location of Merguellil site in Tunisia. The selected 3x3 km² study area.</i>	<i>11</i>
<i>Figure 2: False color composite of the study area. ESUs are located into yellow rectangles.</i>	<i>12</i>
<i>Figure 3: Distribution of the sampling units (ESU) over 5x5 km² area. Orange color: common ESUs in the first and second campaign. (March and May). Green color: ESUs considered only during the second campaign (May).</i>	<i>14</i>
<i>Figure 4: LA_{eff} measurements acquired in Merguellil site during the first campaign of 2013.</i>	<i>16</i>
<i>Figure 5: LA_{eff} measurements acquired in Merguellil site during the second campaign of 2013.</i>	<i>16</i>
<i>Figure 6: Distribution of the measured biophysical variables over the ESUs. Left: First campaign (March). Right: Second campaign (May).</i>	<i>16</i>
<i>Figure 7: Comparison of NDVI distribution between ESUs (green dots) and over the whole image (Blue line). Top: First Campaign (March). Bottom: Second Campaign (May).</i>	<i>18</i>
<i>Figure 8: Convex Hull test over 5x5km² area centered at the test site: blue clear and dark correspond to the pixels belonging to the 'strict' and 'large' convex hulls. Red corresponds to the pixels for which the transfer function is extrapolating and Grey to the soil data filtered with a mask where the transfer function is extrapolating and NDVI value is lower than 0.14. Left: First Campaign (March). Right: Second Campaign (May).</i>	<i>20</i>
<i>Figure 9: Transfer function: Test of multiple regression applied on different band combinations. Band combinations are given in abscissa (2=G, 3=RED, 4=NIR and 5=SWIR). The weighted root mean square error (RMSE) is presented in red along with the cross-validation RMSE in green. The numbers indicate the number of data used for the robust regression with a weight lower than 0.7 that could be considered as outliers. Left: First campaign (March). Right: Second campaign (May).</i>	<i>23</i>
<i>Figure 10: LA_{eff} results for regression on reflectance using 4 and 3 bands combination. Full dots: Weight>0.7. Left: First campaign (March). Right: Second campaign (May).</i>	<i>23</i>
<i>Figure 11: HR LA_{eff} maps (5x5 km²) retrieved on the Merguellil site. Top: First Campaign (March). Bottom: Second Campaign (May).</i>	<i>24</i>
<i>Figure 12: Distribution of the HR LA_{eff} applied on the Merguellil site over the 3x3 km² study area. Left: First campaign (March). Right: Second campaign (May).</i>	<i>25</i>

LIST OF TABLES

<i>Table 1: Coordinates and altitude of the test site.</i>	<i>11</i>
<i>Table 2: The File template used to describe ESUs with the ground measurements.</i>	<i>15</i>
<i>Table 3: Summary of the field measurements in Merguellil site.</i>	<i>15</i>
<i>Table 4: Acquisition geometry of SPOT4 HRVIR XS N2A data used for retrieving high resolution maps.</i>	<i>21</i>
<i>Table 5: Transfer function applied to the whole site for LA_{eff} for weighted RMSE (RW), and RC for cross-validation RMSE.</i>	<i>22</i>
<i>Table 6: Mean values and standard deviation (STD) of the HR LA_{eff} maps for the 3x3km² and 5x5km² Merguellil site.</i>	<i>25</i>
<i>Table 7: Content of the dataset.</i>	<i>25</i>

1. BACKGROUND OF THE DOCUMENT

1.1. EXECUTIVE SUMMARY

The Copernicus Land Service has been built in the framework of the FP7 geoland2 project, which has set up pre-operational infrastructures. ImagineS intends to ensure the continuity of the innovation and development activities of geoland2 to support the operations of the global land component of the GMES Initial Operation (GIO) phase. In particular, the use of the future Sentinel data in an operational context will be prepared. Moreover, IMAGINES will favor the emergence of new downstream activities dedicated to the monitoring of crop and fodder production.

The main objectives of ImagineS are to (i) improve the retrieval of basic biophysical variables, mainly LAI, FAPAR and the surface albedo, identified as Terrestrial Essential Climate Variables, by merging the information coming from different Sentinel sensors and other Copernicus contributing missions; (ii) develop qualified software able to process multi-sensor data at the global scale on a fully automatic basis; (iii) propose an original agriculture service relying upon a new method to assess the biomass, based on the assimilation of satellite products in a Land Data Assimilation System (LDAS) in order to monitor the crop/fodder biomass production together with the carbon and water fluxes; (iv) demonstrate the added value of this agriculture service for a community of users acting at global, European, national, and regional scales.

Further, ImagineS will serve the growing needs of international (e.g. FAO and NGOs), European (e.g. DG AGRI, EUROSTATS, DG RELEX), and national users (e.g. national services in agro-meteorology, ministries, group of producers, traders) on accurate and reliable information for the implementation of the EU Common Agricultural Policy, of the food security policy, for early warning systems, and trading issues. ImagineS will also contribute to the Global Agricultural Geo-Monitoring Initiative (GEO-GLAM) by its original agriculture service which can monitor crop and fodder production together with the carbon and water fluxes and can provide drought indicators, and through links with JECAM (Joint Experiment for Crop Assessment and Monitoring).

1.2. PORTFOLIO

The ImagineS portfolio contains global and regional biophysical variables derived from multi-sensor satellite data, at different spatial resolutions, together with agricultural indicators, including the above-ground biomass, the carbon and water fluxes, and drought indices resulting from the assimilation of the biophysical variables in the Land Data Assimilation System (LDAS). The ambition of the project is to provide a full coverage of the globe, at a frequency of 10 days, merging Sentinel-3 and Proba-V data.

1.3. SCOPE AND OBJECTIVES

The main objective of this document is to describe the ground database provided by the CESBIO - Centre d'Etudes Spatiales de la Biosphère, in order to characterize the cereal crops and the processing carried out by EOLAB to derive high resolution maps of the following biophysical variable:

- Leaf Area Index: One LA_{eff} map is produced per campaign, in which the LA_{eff} (Effective LAI) is derived from hemispherical digital photography (indirect method). A binary classification of green elements and soil is proposed, in order to compute the gap fraction at a 57.5° zenith angle, from which an estimation of the LA_{eff} is then derived.

1.4. CONTENT OF THE DOCUMENT

This document is structured as follows:

- Chapter 2 provides an introduction to the field experiment.
- Chapter 3 provides the location and description of the site.
- Chapter 4 describes the ground measurements, including material and methods, sampling and data processing.
- Chapter 5 describes an evaluation of the sampling.
- Chapter 6 describes the methodology to derive high resolution maps of the biophysical variables, and the results of the high resolution dataset.
- Finally, conclusions and references are given.

2. INTRODUCTION

Validation of remote sensing products is mandatory to guaranty that the satellite products meets the user's requirements. Protocols for validation of global LAIeff products are already developed in the context of Land Product Validation (LPV) group of the Committee on Earth Observation Satellite (CEOS) for the validation of satellite-derived land products (Fernandes et al., 2014), and recently applied to Copernicus global land products based on SPOT/VGT observation (Camacho et al., 2013). This generic approach is made of 2 major components:

- The indirect validation: including inter-comparison between products as well as evaluation of their temporal and spatial consistency
- The direct validation: comparing satellite products to ground measurements of the corresponding biophysical variables. In the case of low and medium resolution sensors, the main difficulty relies on scaling local ground measurements to the extent corresponding to pixels size. However, the direct validation is limited by the small number of sites, for that reason a main objective of ImagineS is the collection of ground truth data in demonstration sites.

The content of this document is compliant with existing validation guidelines (for direct validation) as proposed by the CEOS LPV group (Morissette et al., 2006); the VALERI project (<http://w3.avignon.inra.fr/valeri/>) and ESA campaigns (Baret and Fernandes, 2012). It therefore follows the general strategy based on a bottom up approach: it starts from the scale of the individual measurements that are aggregated over an elementary sampling unit (ESU) corresponding to a support area consistent with that of the high resolution imagery used for the upscaling of ground data. Several ESUs are sampled over the site. Radiometric values over a decametric image are also extracted over the ESUs. This will be later used to develop empirical transfer functions for up-scaling the ESU ground measurements (e.g. Martínez et al., 2009). Finally, the high resolution ground based map will be compared with the medium resolution satellite product at the spatial support of the product.

Two field campaigns to characterize the vegetation biophysical parameters at the Merguellil test site were carried out by the CESBIO - Centre d'Etudes Spatiales de la Biosphère in the framework of METASIM and RESAMED in the SCIMED/MISTRALS French program and AMETHYST in the TRANSMED-ANR program.

First campaign: 8th of March 2013.

Second campaign: 3rd of May 2013.

Team involved in field collection:

Mehrez Zribi , Hassan Ayari, Bernard Mougnot (CESBIO)

Aicha Chahbi (CESBIO-INAT)

Contact: Mehrez Zribi (mehrez.zribi@ird.fr)

3. STUDY AREA

3.1. LOCATION

The experimental Merguellil site is located around the Kairouan plain, situated in central Tunisia (9°30'E-10°15'E, 35°N, 35°45'N). The climate in this region is semi-arid, with an average annual rainfall of approximately 300 mm per year, characterized by a rainy season lasting from October to May, with the two rainiest months being October and March. As is generally the case in semi-arid areas, the rainfall patterns in this area are highly variable in time and space. The mean temperature in Kairouan City is 19.2°C (minimum of 10.7° in January and maximum of 28.6°C in August). The mean annual potential evapotranspiration (Penman) is close to 1600mm.



Figure 1: Location of Merguellil site in Tunisia. The selected 3x3 km² study area.

The study area (Figure 1) is defined by a 3x3 km² region around the central coordinate (Table 1). The maps have been generated for a bigger area, 5x5 km² in order to cover all the selected fields.

Table 1: Coordinates and altitude of the test site.

Site Center	
Geographic Lat/Ion, WGS-84 (degrees)	Latitude = 35°33'58.38" N Longitude = 9°54'43.78" E
Altitude	127 m

3.2. DESCRIPTION OF THE TEST SITE.

The landscape is mainly flat and the vegetation in this area is dominated by agriculture (cereals, olive trees, and market gardens). Crops types are wheat, tomatoes, pepper, broad beans, melon, watermelon and olive. Typical field rotation is cereals, forage, broad beans in winter, and vegetables in summer. Land cover changes are observed in some fields plots (Figure 2).

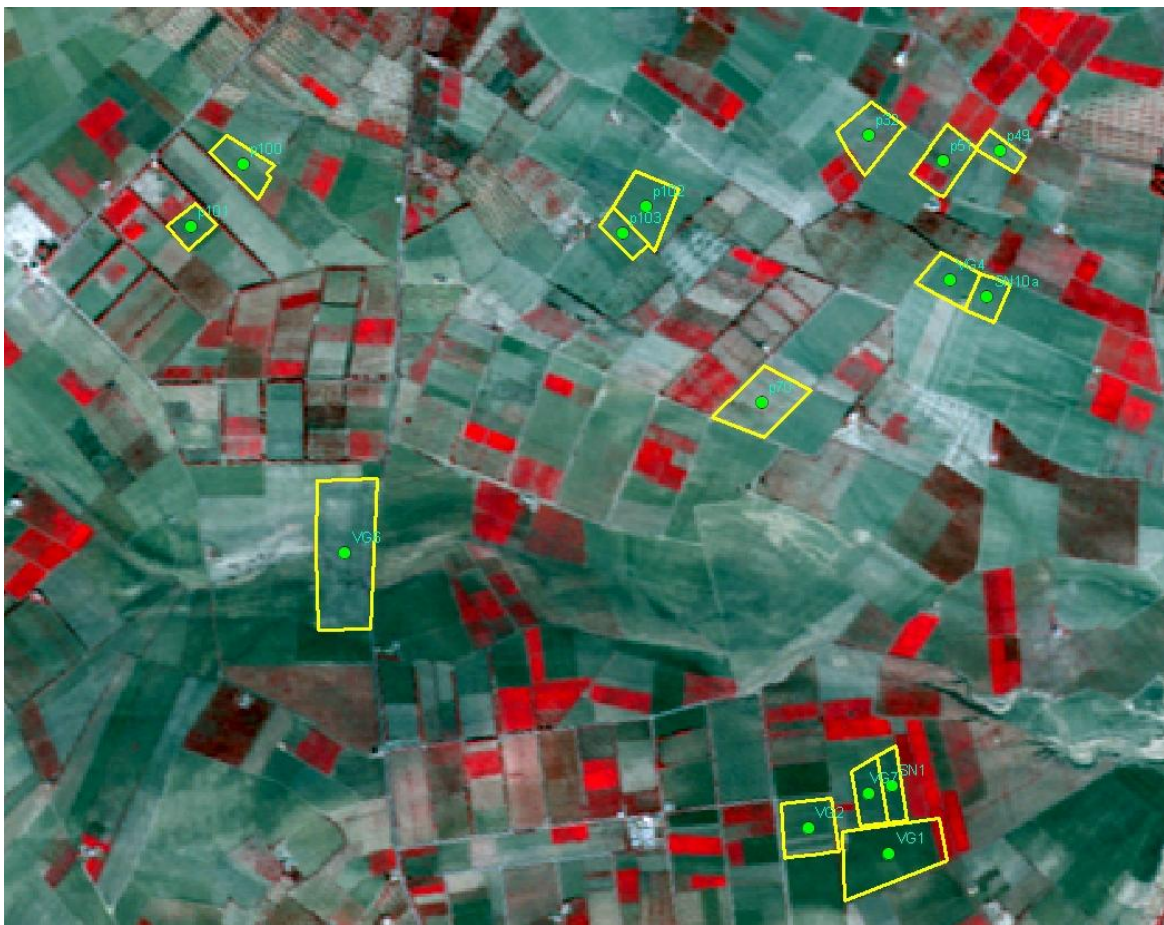


Figure 2: False color composite of the study area. ESUs are located into yellow rectangles.

The crop calendar is winter wheat (dec-june), spring vegetables (march-july) summer vegetables (june-october), trees all year (olive). Their rotation is typical of semi-arid regions. The aquifer of the Kairouan plain represents the largest basin in central Tunisia. It is fed by the infiltration of surface waters during floods in the natural regime, or at the time of dam releases since the construction of the Sidi Saad and El Houareb dams. Surface and groundwater streams drain into the Sebkhia Kelbia, a large salt lake.

4. GROUND MEASUREMENTS

The ground measurement database was acquired and provided by the CESBIO - Centre d'Etudes Spatiales de la Biosphère.

4.1. MATERIAL AND METHODS

In the present study, an indirect method is used, in which the LA_{eff} is derived from hemispherical digital photography. A binary classification of green elements and soil is proposed, in order to compute the gap fraction at a 57.5° zenith angle, from which an estimation of the LA_{eff} is then derived (Demarez et al., 2008).

Digital Hemispheric Photographs (DHP) were acquired with a digital camera. Hemispherical photos allow the calculation of LA_{eff} measuring gap fraction through an extreme wide-angle camera lens (i.e. 180°) (Weiss et al., 2004). It produces circular images that record the size, shape, and location of gaps, either looking upward from within a canopy or looking downward from above the canopy. The hemispherical images acquired during the field campaign are processed with the CAN-EYE software (http://www.avignon.inra.fr/can_eye) to derive LA_{eff}. It is based on a RGB colour classification of the image to discriminate vegetation elements from background (i.e., gaps).

These measurements were applied to each cereal field, on different days during the vegetation season.

4.2. SPATIAL SAMPLING SCHEME

A total of 14 (18) ESUs were characterized during the first (second) campaign. A pseudo-regular sampling was used within each ESU of approximately 20x20 m². The centre of the ESU was geo-located using a GPS. The number of hemispherical photos per ESU ranges between 12 and 15.

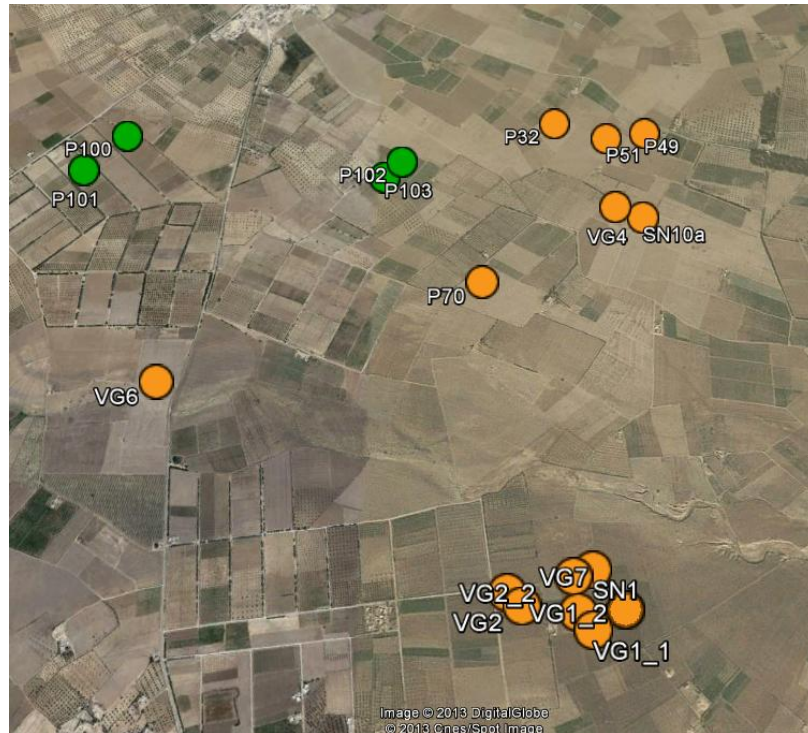


Figure 3: Distribution of the sampling units (ESU) over 5x5 km² area. Orange color: common ESUs in the first and second campaign. (March and May). Green color: ESUs considered only during the second campaign (May).

4.3. CONTENT OF THE GROUND DATASET

Each ESU is described according to an agreed format. For this purpose a template file has been used (Table 2).

Table 3 summarizes the number of sampling units (ESUs) per each crop type acquired during the two field campaigns.

Table 2: The File template used to describe ESUs with the ground measurements.

Column	Var.Name	Comment
1	Plot #	Number of the field plot in the site
2	Plot Label	Label of the plot in the site
3	ESU #	Number of the Elementary Sampling Unit (ESU)
4	ESU Label	Label of the ESU in the campaign
5	Northing Coord.	Geographical coordinate: Latitude (°), WGS-84
6	Easting Coord.	Geographical coordinate: Longitude (°), WGS-84
7	Extent (m) of ESU (diameter)	Size of the ESU ⁽¹⁾
8	Land Cover	Detailed land cover
9	Start Date (dd/mm/yyyy)	Starting date of measurements
10	End Date (dd/mm/yyyy)	Ending date of measurements
11	LA _{eff}	Method
12		Nb. Replications
13		PRODUCT
14		Uncertainty
		Instrument
		Number of Replications
		Methodology
		Standard deviation

Table 3: Summary of the field measurements in Merguellil site.

ESU internal code	Number of ESU's	
	First Campaign (8 th of March, 2013)	Second Campaign (3 rd of May, 2013)
VG	8	8
SN	2	2
P	4	8
TOTAL	14	18

Figures 4, and 5 show the measurements obtained during the field experiment. Figure 6 shows the distribution of measurements. Distribution of LA_{eff} values varies from 0 to 5.5 for the first campaign and from 0 to 1.7 for the second campaign.

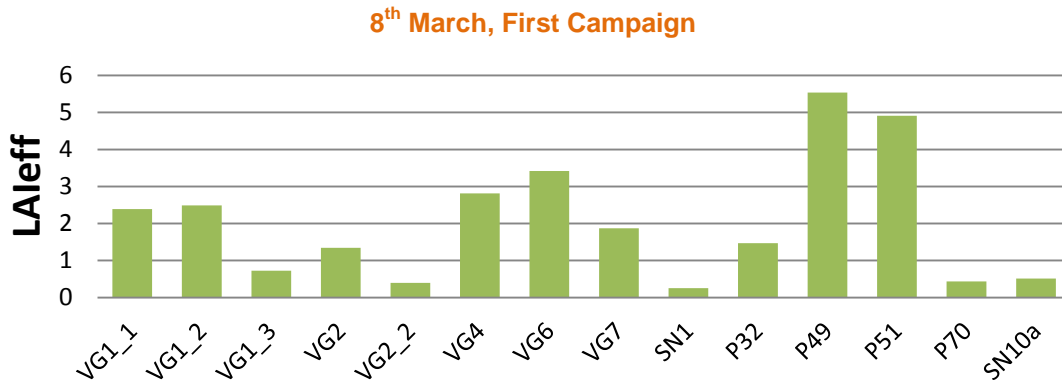


Figure 4: LAleff measurements acquired in Merguellil site during the first campaign of 2013.

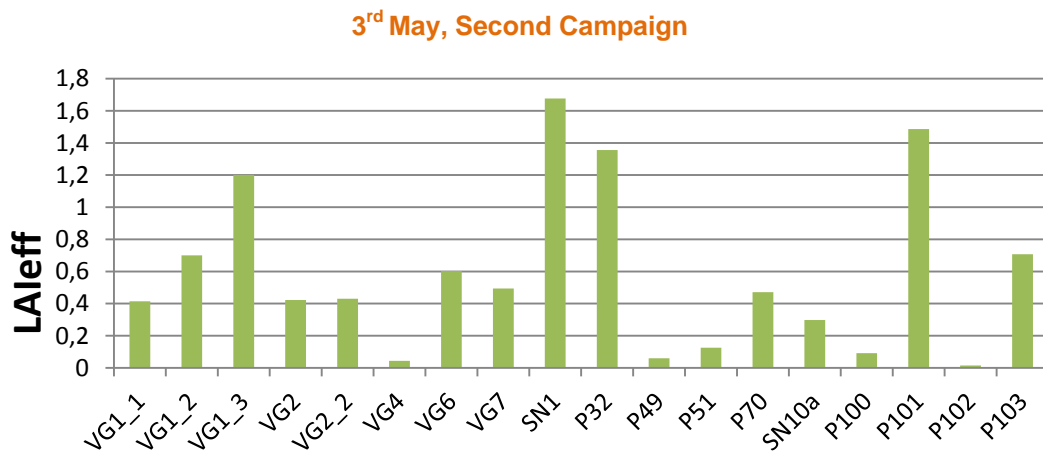


Figure 5: LAleff measurements acquired in Merguellil site during the second campaign of 2013.

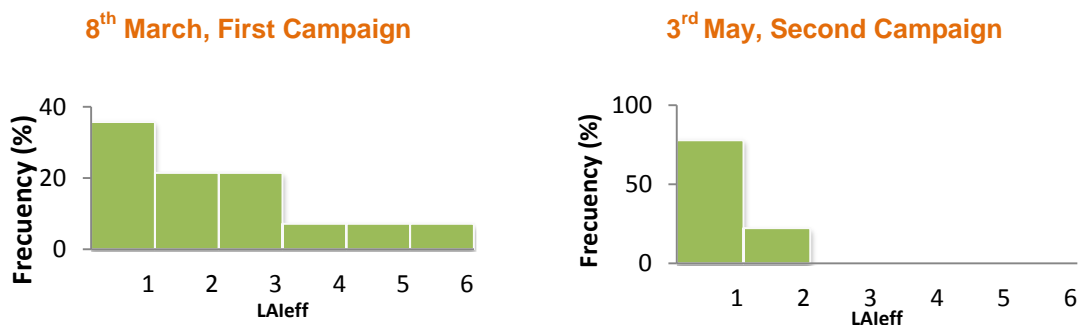


Figure 6: Distribution of the measured biophysical variables over the ESUs. Left: First campaign (March). Right: Second campaign (May).

5. EVALUATION OF THE SAMPLING

5.1. PRINCIPLES

Based on previous field activities, the data set sampling was concentrated in the most representative crops. The number of ESUs was of 14 and 18 for the first and second campaigns respectively.

5.2. EVALUATION BASED ON NDVI VALUES

The sampling strategy is evaluated using the SPOT4 image by comparing the NDVI distribution over the site with the NDVI distribution over the ESUs (Figure 7). As the number of pixels is drastically different for the ESU and whole site (WS) it is not statistically consistent to directly compare the two NDVI histograms. Therefore, the proposed technique consists in comparing the NDVI cumulative frequency of the two distributions by a Monte-Carlo procedure which aims at comparing the actual frequency to randomly shifted sampling patterns. It consists in:

1. computing the cumulative frequency of the N pixel NDVI that correspond to the exact ESU locations; then, applying a unique random translation to the sampling design (modulo the size of the image)
2. computing the cumulative frequency of NDVI on the randomly shifted sampling design
3. repeating steps 2 and 3, 199 times with 199 different random translation vectors.

This provides a total population of $N = 199 + 1$ (actual) cumulative frequency on which a statistical test at acceptance probability $1 - \alpha = 95\%$ is applied: for a given NDVI level, if the actual ESU density function is between two limits defined by the $N\alpha / 2 = 5$ highest and lowest values of the 200 cumulative frequencies, the hypothesis assuming that WS and ESU NDVI distributions are equivalent is accepted, otherwise it is rejected.

Figure 7 shows that the NDVI distribution of the first campaign (top) is good over the whole site (comprised between the 5 highest and lowest cumulative frequencies). The first campaign over this site is very heterogeneous in terms of NDVI since the lowest and the highest distributions are very different. For the second campaign, figure 7 (bottom) shows that the NDVI distribution for low vegetation cover (NDVI lower 0.3) the sampling presents a bias towards low NDVI values.

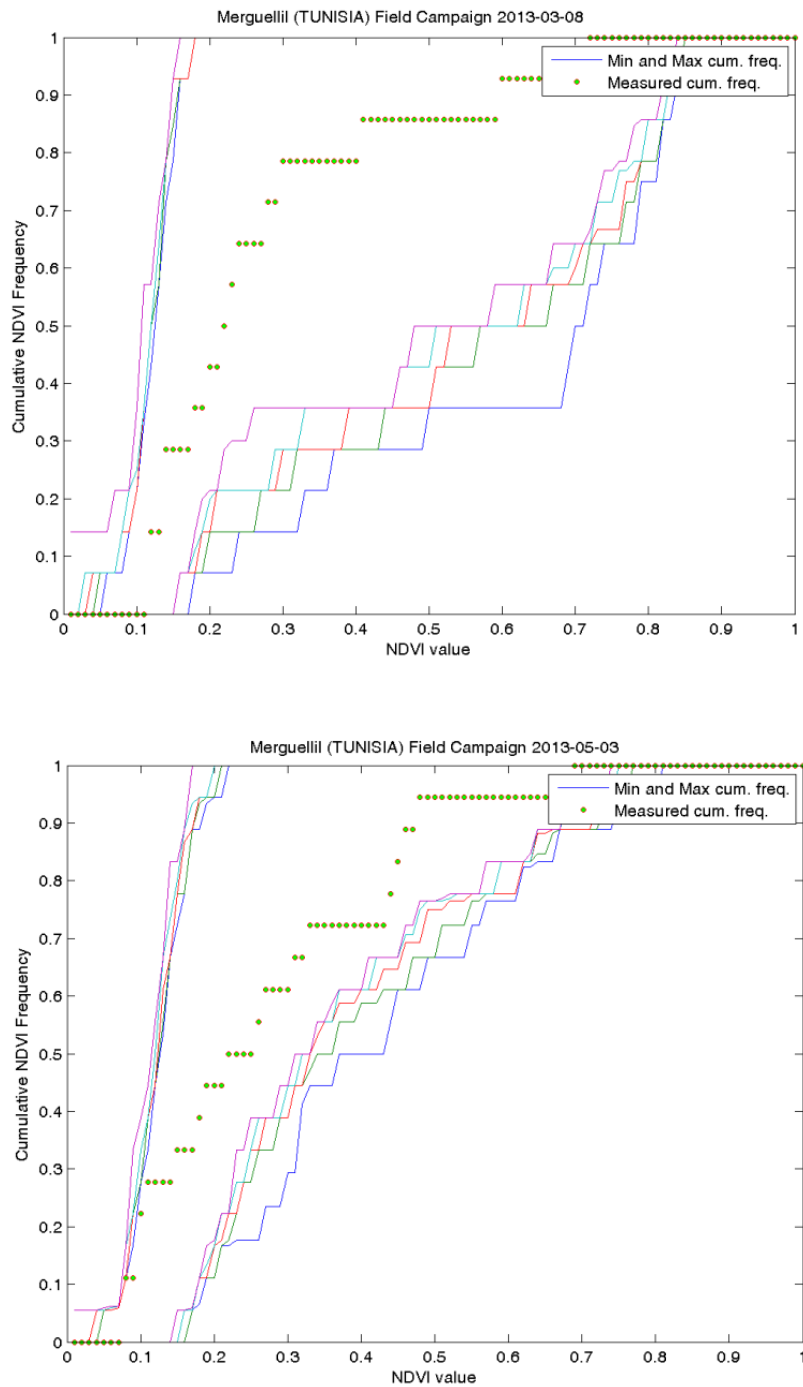


Figure 7: Comparison of NDVI distribution between ESUs (green dots) and over the whole image (Blue line). Top: First Campaign (March). Bottom: Second Campaign (May).

5.3. EVALUATION BASED ON CONVEX HULL: PRODUCT QUALITY FLAG.

The interpolation capabilities of the empirical transfer function used for up-scaling the ground data using decametric images is dependent of the sampling (Martinez et al., 2009). A test based on the convex hulls was also carried out to characterize the representativeness of ESUs and the reliability of the empirical transfer function using the different combinations of the selected bands (green, red, NIR and SWIR) of the SPOT4 image. A flag image is computed over the reflectances. The result on convex-hulls can be interpreted as:

- pixels inside the 'strict convex-hull': a convex-hull is computed using all the SPOT4 reflectances corresponding to the ESUs belonging to the class. These pixels are well represented by the ground sampling and therefore, when applying a transfer function the degree of confidence in the results will be quite high, since the transfer function will be used as an interpolator;

- pixels inside the 'large convex-hull': a convex-hull is computed using all the reflectance combinations ($\pm 5\%$ in relative value) corresponding to the ESUs. For these pixels, the degree of confidence in the obtained results will be quite good, since the transfer function is used as an extrapolator (but not far from interpolator);

- pixels outside the two convex-hulls: this means that for these pixels, the transfer function will behave as an extrapolator which makes the results less reliable. However, having a priori information on the site may help to evaluate the extrapolation capacities of the transfer function.

The Figure 8 shows the results of the Convex-Hull test (i.e., Quality Flag image) for the Merguellil site over a $5 \times 5 \text{ km}^2$ area around the central coordinate site. The flag maps show also that there is a big extrapolation of the transfer function all over the site as shown by the test on the sampling strategy. The strict and large convex-hulls are poor in a $3 \times 3 \text{ km}^2$ area (10% and 26%).

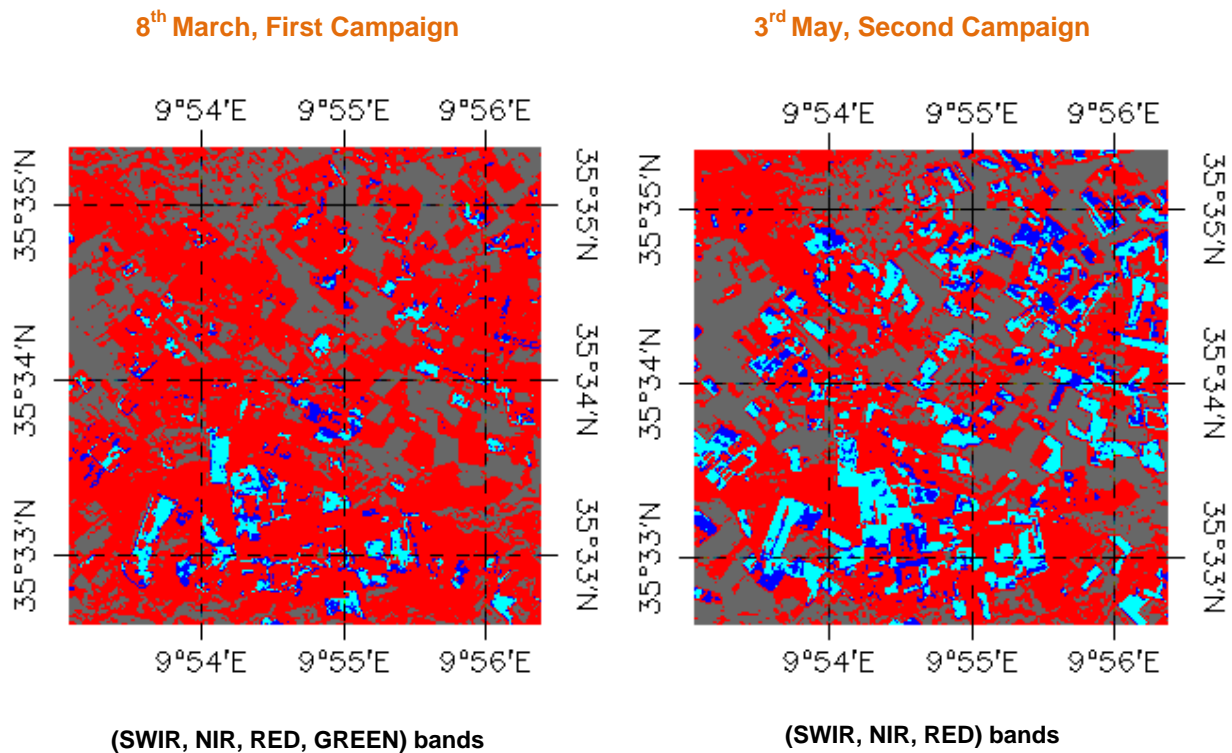


Figure 8: Convex Hull test over 5x5km² area centered at the test site: blue clear and dark correspond to the pixels belonging to the 'strict' and 'large' convex hulls. Red corresponds to the pixels for which the transfer function is extrapolating and Grey to the soil data filtered with a mask where the transfer function is extrapolating and NDVI value is lower than 0.14. Left: First Campaign (March). Right: Second Campaign (May).

6. ESTIMATION OF THE HIGH RESOLUTION MAPS

6.1. IMAGERY

The SPOT4 images were acquired the 10th March and 4th May 2013 (see Table 4 for acquisition geometry). It corresponds to 4 spectral bands from 500 nm to 1750 nm with a nadir ground sampling distance of 20 m. Therefore, for the transfer function analysis, the input satellite data used is Top of Canopy (TOC) reflectance. The original projection is UTM 32 North, WGS-84.

Table 4: Acquisition geometry of SPOT4 HRVIR XS N2A data used for retrieving high resolution maps.

SPOT 4 METADATA		
Platform / Instrument	SP04 / HRVIR XS	
Sensor	OPTICAL 20 m	
Spectral Range	B1(green) : 0.5-0.59 μm B2(red) : 0.61-0.68 μm B3(NIR) : 0.78-0.89 μm B4(SWIR) : 1.58-1.75 μm	
	First Campaign	Second Campaign
Acquisition date	2013-03-10 09:18:53.25	2013-05-04 09:14:15.75
Phi- solar angle	135.02°	117.53°
Theta- solar angle	50.82°	33.99°
Phi-View angle	-77.47°	-77.48°
Theta-View angle	23.15°	23.14°

6.2. THE TRANSFER FUNCTION

6.2.1. The regression method

If the number of ESUs is enough, multiple robust regression 'REG' between ESUs reflectance and the considered biophysical variable can be applied (Martínez et al., 2009): we used the 'robustfit' function from the Matlab statistics toolbox. It uses an iteratively re-weighted least squares algorithm, with the weights at each iteration computed by applying the bi-square function to the residuals from the previous iteration. This algorithm provides lower weight to ESUs that do not fit well.

The results are less sensitive to outliers in the data as compared with ordinary least squares regression. At the end of the processing, two errors are computed: weighted RMSE (using the weights attributed to each ESU) and cross-validation RMSE (leave-one-out method).

As the method has limited extrapolation capacities, a flag image (Figure 8), based on the convex hulls, is included in the final ground based map in order to inform the users on the reliability of the estimates.

6.2.2. Band combination

Figure 9 shows the results obtained for all the possible band combinations using the reflectance. Attending specifications of minimal noise and maximal sensitivity it has been chosen for the first campaign (8th March): band 1 (green), band 2 (red) band 3 (Near Infrared) and band 4 (Short Wave Infrared) combination of (1,2,3,4) = (G, R, N, S). For the second campaign (3rd May), the 3 selected bands are band 2 (red), band 3(Near Infrared) and band 4 (Short Wave Infrared), the combination (2, 3, 4) = (R, NIR, SWIR).

These combinations on reflectance were selected since provide a good compromise between the cross-validation RMSE, the weighted RMSE (lowest value) and the number of rejected points.

6.2.3. The selected Transfer Function

The applied transfer function is detailed in Table 5, along with its weighted and cross validated errors.

Table 5: Transfer function applied to the whole site for LA_{eff} for weighted RMSE (RW), and RC for cross-validation RMSE.

Variable	Band Combination	RW	RC
First Campaign			
LA_{eff}	$-2.211+0.0067 \cdot (\text{SWIR})-0.0025 \cdot (\text{NIR})$ $-0.147 \cdot (\text{R})+0.189 \cdot (\text{G})$	1.42	1.48
Second Campaign			
LA_{eff}	$-0.317-0.011 \cdot (\text{SWIR})+0.001 \cdot (\text{NIR})-0.019 \cdot (\text{R})$	0.47	0.52

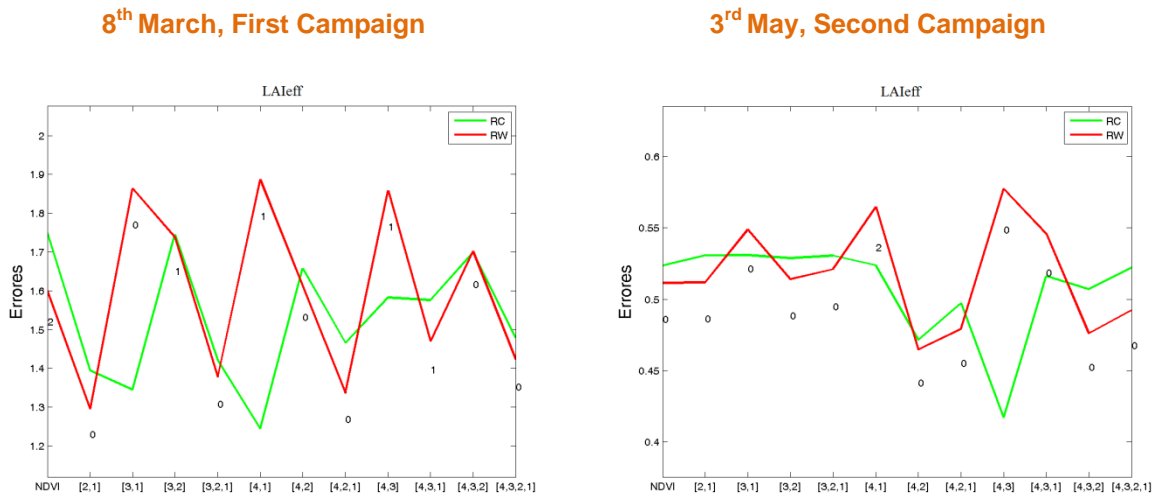


Figure 9: Transfer function: Test of multiple regression applied on different band combinations. Band combinations are given in abscissa (2=G, 3=RED, 4=NIR and 5=SWIR). The weighted root mean square error (RMSE) is presented in red along with the cross-validation RMSE in green. The numbers indicate the number of data used for the robust regression with a weight lower than 0.7 that could be considered as outliers. Left: First campaign (March). Right: Second campaign (May).

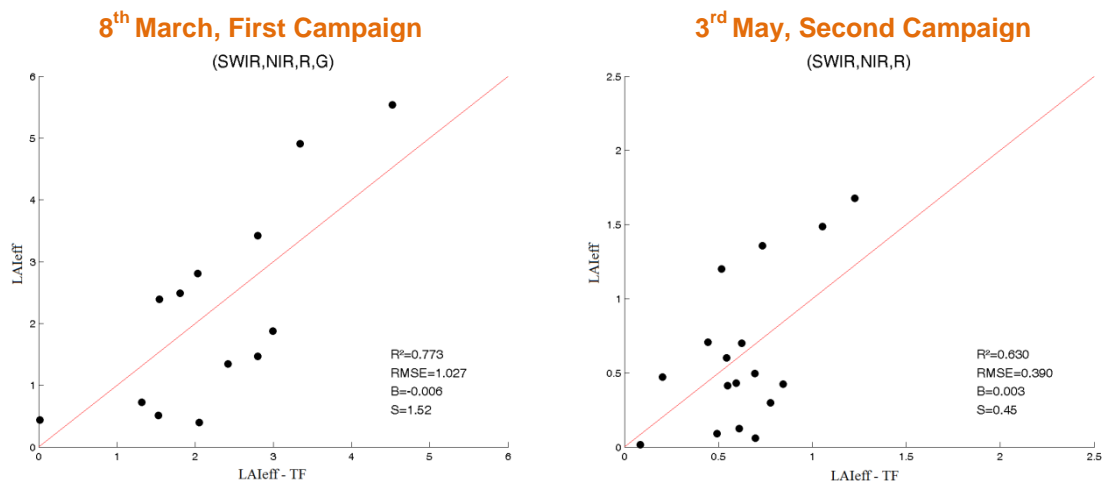


Figure 10: LAleff results for regression on reflectance using 4 and 3 bands combination. Full dots: Weight>0.7. Left: First campaign (March). Right: Second campaign (May).

Figure 10 shows scatter-plots between ground observations and their corresponding transfer function (TF) estimates for the selected bands combinations. For the first campaign, a good correlation is observed for the LAleff with points distributed along the 1:1 line. However, for the second campaign the TF estimates present less variability than the ground observations.

6.3. THE HIGH RESOLUTION GROUND BASED MAPS

The high resolution maps are obtained applying the selected transfer function (Table 5) to the SPOT4 TOC reflectance. Figure 11 presents the TF biophysical variables over a 5x5 km² area. Figure 8 shows the Quality Flag included in the final product.

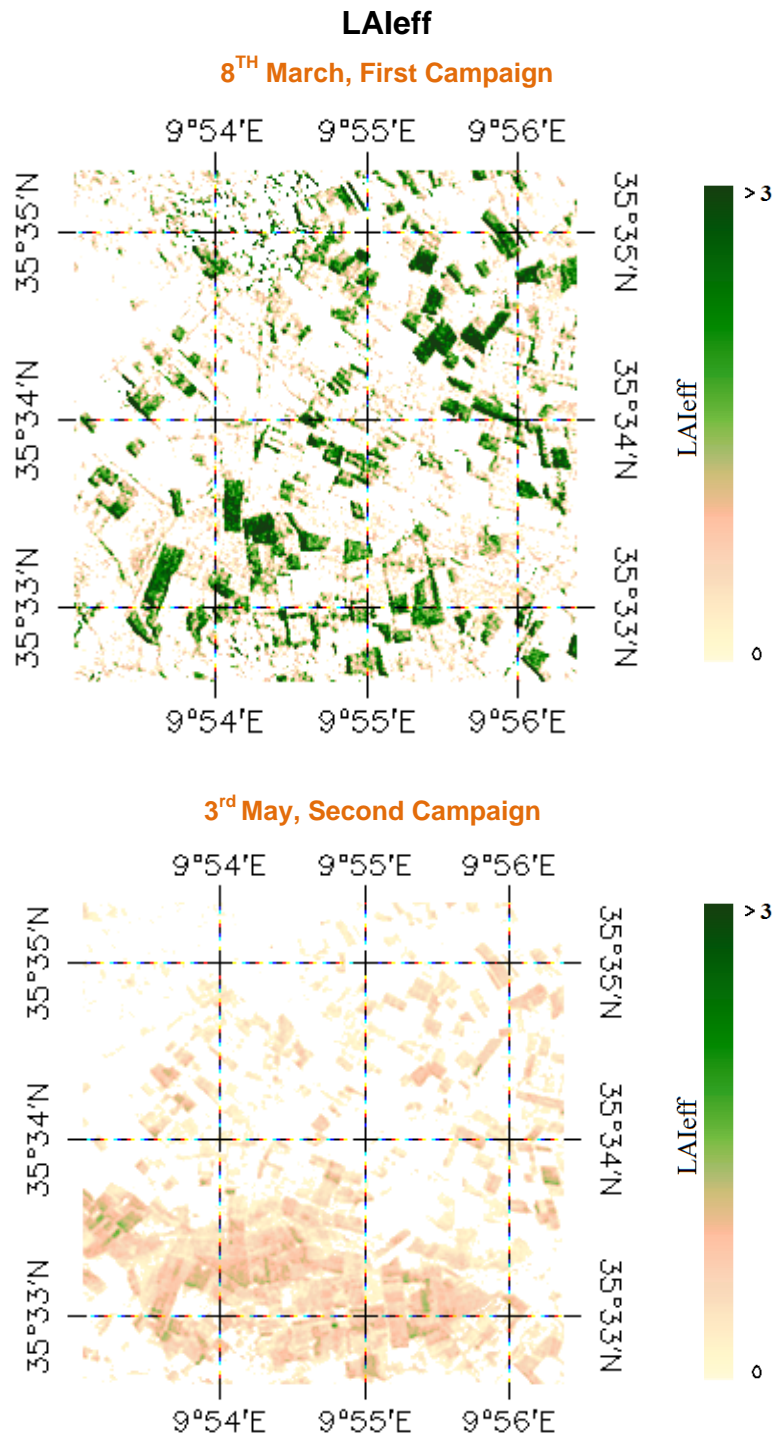


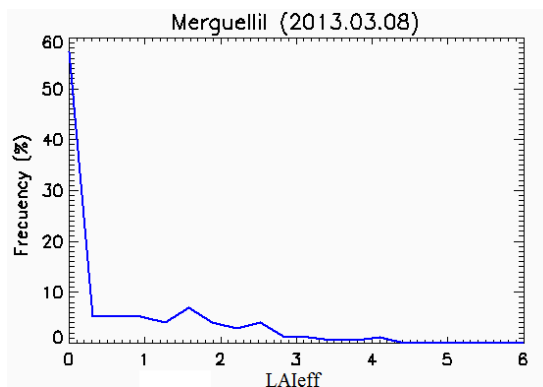
Figure 11: HR LA_{leff} maps (5x5 km²) retrieved on the Merguellil site. Top: First Campaign (March). Bottom: Second Campaign (May).

Table 6 summarizes the mean values for the 5x5 km² and 3x3 km² study area with the same centre. Both maps as the mean values (Table 6), a systematic decrease of the vegetation is observed according to the phenology of the region. Figure 12 shows the distribution of values for the 3x3 km² study area. The distributions of biophysical maps are consistent with field measurements distributions (figure 6).

Table 6: Mean values and standard deviation (STD) of the HR LA_{eff} maps for the 3x3km² and 5x5km² Merguellil site.

Variable (area)	First Campaign		Second Campaign	
	Mean	STD	Mean	STD
LA _{eff} (5x5 km ²)	0.431	0.829	0.176	0.289
LA _{eff} (3x3 km ²)	0.477	0.862	0.195	0.291

8th March, First Campaign



3rd May, Second Campaign

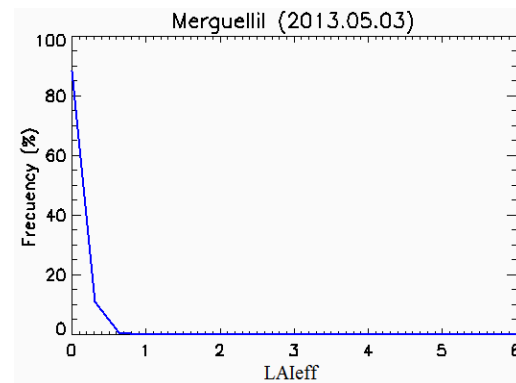


Figure 12: Distribution of the HR LA_{eff} applied on the Merguellil site over the 3x3 km² study area. Left: First campaign (March). Right: Second campaign (May).

Table 7 describes the content of the geo-biophysical maps in the “SPOT_YYMMDD_Merguellil_AREA ETF_BioMap” files.

Table 7: Content of the dataset.

Parameter	Dataset name	Range	Variable Type	Scale Factor	No Value
LA _{eff}	LA _{eff}	[0, 7]	Integer	1000	-1
Quality Flag	QFlag	0,1,2,3 (*)	Integer	N/A	-1

(*) 0 means extrapolated value (low confidence), 1 strict interpolator (best confidence), 2 large interpolator (medium confidence), 3 soil values

7. CONCLUSIONS

High resolution maps of the biophysical variable LA_{eff} have been derived over the agriculture area of Merguellil (Tunisia) for 8th of March and 3rd of May, 2013. Ground data was acquired using digital hemispherical photographs, and processed with CAN-EYE to provide LA_{eff} values. Ground based maps have been derived using high resolution imagery (SPOT- 4) according with the CEOS LPV recommendations for validation of low resolution satellite sensors.

The sampling over the study area of Merguellil site is limited over vegetated crop (between 14 - 18 ESUs) and for this site a soil mask has been applied based on NDVI threshold (< 0.14). According to the convex hull test, only 33 % of the total Merguellil test site (3x3 km²) area belongs to the transfer function considered as an interpolator or soil mask for the first campaign and 51 % for the second one. Thus, the representativeness of the sampling for the first campaign is low resulting in lower confidence of the transfer function estimates.

The RMSE values are between 1.027 and 0.390 of LA_{eff} In-situ measurements for the first and second campaign. Attending optimal characteristics of noise and sensitivity, different combinations of bands have been chosen, for the first campaign (8th March): band 1 (green), band 2 (red) band 3 (Near Infrared) and band 4 (Short Wave Infrared) combination, and for the second campaign (3rd May), the selected bands are band 2 (red), band 3(Near Infrared) and band 4 (Short Wave Infrared).

The biophysical variable maps are available in geographic (latitude-longitude projection WGS-84) coordinates at 20m resolution. The spatial and spectral analysis of the high biophysical maps has been carried out by calculating means and standard deviation for LA_{eff}.

Despite of the study area involves 3x3km², the maps have been extended to a larger region, 5x5 km² in order to cover all the fields. The 3x3 km² mean values obtained for first and second campaign are respectively: 0.477 and 0.195. The distribution of values of high resolution maps were found consistent with the ground sampling, according to the phenology of the site.

8. ACKNOWLEDGEMENTS

This work is supported by the FP7 IMAGINES project under Grant Agreement N°311766. SPOT 4-HRVIR XS images are download through the TAKE-5 Experiment (CNES Space for Earth Services, from [THEIA](http://spirit.cnes.fr/take5/) distribution website <http://spirit.cnes.fr/take5/>).

Thanks to the CESBIO - Centre d'Etudes Spatiales de la BIOsphère (Unité Mixte de Recherche (CNRS, UPS, CNES, IRD)) for providing the field data. These activities were carried in the context of two projects METASIM and RESAMED in the SICMED/MISTRALS French program and AMETHYST in the TRANSMED-ANR program.

9. REFERENCES

- Baret, F and Fernandes, R. (2012). Validation Concept. VALSE2-PR-014-INRA, 42 pp.
- Camacho, F., Cernicharo, J., Lacaze, R., Baret, F., and Weiss, M. (2013). GEOV1: LAI, FAPAR Essential Climate Variables and FCOVER global time series capitalizing over existing products. Part 2: Validation and intercomparison with reference products. *Remote Sensing of Environment*, 137: 310-329.
- Demarez, V., Duthoit, S., Baret, F., Weiss, M. and Dedieu, G. (2008). Estimation of leaf area and clumping indexes of crops with hemispherical photographs. *Agricultural and Forest Meteorology*. 148, 644-655.
- Fernandes, R., Plummer, S., Nightingale, J., et al. (2014). Global Leaf Area Index Product Validation Good Practices. CEOS Working Group on Calibration and Validation - Land Product Validation Sub-Group. *Version 2.0: Public version made available on LPV website*.
- Martínez, B., García-Haro, F. J., & Camacho, F. (2009). Derivation of high-resolution leaf area index maps in support of validation activities: Application to the cropland Barrax site. *Agricultural and Forest Meteorology*, 149, 130–145.
- Morisette, J. T., Baret, F., Privette, J. L., Myneni, R. B., Nickeson, J. E., Garrigues, S., et al. (2006). Validation of global moderate-resolution LAI products: A framework proposed within the CEOS land product validation subgroup. *IEEE Transactions on Geoscience and Remote Sensing*, 44, 1804–1817.
- Weiss, M., Baret, F., Smith, G.J., Jonckheere, I. and Coppin, P., (2004). Review of methods for in situ leaf area index (LAI) determination. Part II. Estimation of LAI, errors and sampling. *Agricultural and Forest Meteorology*. 121, 37–53.